JOURNAL OF PETROLOGY | VOLUME 39 | NUMBER 7 | PAGES 1307–1323 | 1998

Origin of Anorthosite by Textural Coarsening: Quantitative Measurements of a Natural Sequence of Textural Development

MICHAEL D. HIGGINS*

SCIENCES DE LA TERRE, UNIVERSITÉ DU QUÉBEC À CHICOUTIMI, CHICOUTIMI, G7H 2B1, CANADA

RECEIVED JULY 16, 1997; REVISED TYPESCRIPT ACCEPTED FEBRUARY 3, 1998

The textures of plagioclase crystals within large olivine oikocrysts preserve the sequence of the formation of anorthosite. Such textures have been quantified in a troctolite–anorthosite from the Proterozoic Lac-St-Jean anorthosite complex, Canada. Crystal size distributions (CSDs) indicate that initially plagioclase nucleated and grew in an environment of linearly increasing undercooling, producing a straight-line CSD. During this phase, latent heat of crystallization was largely removed by circulation of magma through the porous crystal mush. By about 25% solidification the crystallinity was such that it reduced, but did not eliminate, the circulation of magma, resulting in the retention of more latent heat within the crystal pile. The temperature rose until it was buffered by the solution of plagioclase close to the liquidus temperature of plagioclase. Nucleation of plagioclase was inhibited and conditions were suitable for textural coarsening of both plagioclase and olivine to occur (Ostwald ripening). In this process small crystals were resorbed, whereas larger crystals grew from both material recycled by the resorption of crystals smaller than the critical size and new material brought in by the circulating magmatic fluid. The results of this process resemble those of high-temperature metasomatism but there is no necessity for a magmatic fluid with a different composition. The shapes of the plagioclase CSDs fit better the communicating neighbours equation of textural coarsening, rather than the classic Lifshitz–Slyozov–Wagner equation, as do other examples drawn from the literature. If olivine started to nucleate at a higher temperature than plagioclase, then during the textural coarsening phase olivine would have been more undercooled than plagioclase, and would have had a higher maximum growth rate. In these conditions olivine would coarsen more rapidly than plagioclase and engulf it. Hence the order of crystallization determined from the textures would be the reverse of the order of first nucleation of the two phases, from equilibrium phase diagrams. Maintenance of the temperature near the plagioclase liquidus may also inhibit the nucleation and growth of other phases.

KEY WORDS: *Ostwald ripening; CSD; plagioclase; texture*

INTRODUCTION

The textures of plutonic rocks are one of their most striking aspects, but they have been little used to elucidate petrological processes as compared with chemical and isotopic methods. Where used, discussion has tended to be qualitative, in contrast to quantitative chemical methods, hence reducing the weight of this approach. Indeed, it is not possible to verify physical models if quantitative data are not available. Quantitative textural studies of volcanic rocks are becoming more common and these methods are applied here to the development of anorthosite.

Quantitative textural studies of plutonic rocks really started with Jackson's studies of the Stillwater complex in 1961 (Jackson, 1961). He measured crystal size distributions, but did not record the area that he measured, hence his data cannot be completely compared with modern data. His pioneering work was not really followed up, and since then most studies have looked only at 'average' or 'typical' crystal sizes. These data are much less revealing of petrological processes than crystal size distributions, partly because they only give one parameter for each sample. The few existing studies of crystal size distributions in plutonic rocks have not treated plagioclase.

One problem especially pertinent to quantitative textural studies is the way that many igneous petrologists look at rocks: they commonly try to reconstruct how a rock has formed by examining the final, fully crystallized

*Currently on sabbatical at the Dept. de Géologie, Université Blaise Pascal, 5 rue Kessler, Clermont-Ferrand 63038, France. e-mail: mhiggins@uqac.uquebec.ca

product [for a recent example applied to anorthosite, see Lafrance *et al.* (1995)]. However, most plutonic rocks probably form by both growth and solution of crystals, hence many aspects of their early history are not evident in the final rock (Boudreau, 1987; Hunter, 1996; Higgins, 1997). Clearly, these processes can only be fully understood by the quantitative analysis of a sequence of textures. Realistic sequences of textural development from nucleation to complete solidification probably cannot be produced in the laboratory, although some aqueous systems may be relevant (Means & Park, 1994). Therefore, we must seek out natural sequences of textural development.

Some oikocrystic plutonic rocks preserve such time sequences: early textures of chadocrysts are seen in oikocrysts, whereas the matrix material between the oikocrysts preserves the later textures (Mathison, 1987; Higgins, 1991, 1997; McBirney & Hunter, 1995). The process is as follows. Oikocrysts grew from the same magma as the chadocrysts but faster, displacing the magma between the crystals. Without a liquid to facilitate chemical transport, grain boundaries of the chadocrysts move slowly and further textural development is inhibited. Hence, textures of chadocrysts in oikocrysts or parts of oikocrysts that grew at different times can preserve a time-sequence of textural development, or at least some aspects of it. Quantitative analysis of the sequence of textures will be applied here to study the origin of anorthosite.

THE LAC-ST-JEAN ANORTHOSITE COMPLEX

The Lac-St-Jean anorthosite complex (LSJAC) is a massif-type body comprising many plutons, which were emplaced from 1157 to 1142 Ma into the central part of the Grenville Province, Canada (Higgins & van Breemen, 1992). Individual plutons vary widely in their degree of deformation, but in every case so far examined geochronological evidence has shown that most of the deformation was synchronous with emplacement. Similarly, metamorphic effects in the LSJAC, such as coronas around mafic minerals and baddeleyite, were produced by heat from later injections of magma, and are hence evidence of contact metamorphism (Higgins & van Breemen, 1992). Thus the LSJAC lacks regionally imposed Grenville metamorphism and deformation, although it must have cooled relatively slowly. Other massif-type anorthosites that have not been subjected to regional metamorphism or deformation show a similar degree of deformation, which is also ascribed to movements associated with emplacement of the pluton and adjacent plutons (Laramie, Wyoming, Lafrance *et al.*, 1995; Nain, Labrador, B. Ryan, personal communication, 1997; Rogaland, Norway, Maijer & Padget, 1989).

The rocks examined here are part of an early (1157 Ma) layered troctolite–anorthosite pluton of the LSJAC, centred on the town of Alma (Woussen *et al.*, 1988; Higgins & van Breemen, 1992). The composition of the rocks and the style of the layering are variable, both on a kilometre and an outcrop scale. The samples were taken from a large, texturally variable outcrop of troctolite and anorthosite located at UTM coordinates 19U 306200 5386400, 5 km NNE of the town of Alma.

The dominant texture is 'Nodular' troctolite, in which amoeboid olivine oikocrysts 10–20 cm in diameter are spaced 20–30 cm apart within a matrix of anorthosite (Woussen *et al.*, 1988; Figs 1 and 2). The oikocrysts consist of a single or possibly a few olivine crystals with abundant chadocrysts of plagioclase. The rest of the rock is dominated by plagioclase, which is commonly massive but locally foliated. Where foliated the fabric is well developed in the oikocrysts and its orientation is the same in adjacent oikocrysts (Fig. 2). The fabric is defined by the shape-preferred orientations of the plagioclase crystals. As most plagioclase crystals are flattened parallel to the albite twin plane the foliation is also defined by the lattice orientations. The foliation is also evident in the plagioclase of the matrix between the oikocrysts, but it is less well developed, although again broadly parallel to that in the oikocrysts. Here the foliation is more defined by the lattice orientations, as revealed by the orientation of the trace of the albite twin lamellae. The direction of lamination in the matrix does not wrap around the oikocrysts, as has been observed in other troctolites (compare Sept Iles Intrusion, Higgins, 1991).

Elsewhere on this outcrop other textures are present. The Nodular Troctolite is transitional to fine-scale layering (Fig. 1): the oikocrysts become flatter, smaller and more numerous until they are comparable in size with the plagioclase crystals. Layers repeat at 3–10 cm intervals. Both plagioclase and olivine are similar in size to the plagioclase of the Nodular Troctolite matrix. The plagioclase is not laminated. Both types of troctolite are abruptly transitional to pure anorthosite. The troctolite–anorthosite contacts cut across layering in broad sinuous curves. The pure anorthosite resembles the matrix of the Nodular Troctolite and the anorthosite layers of the layered troctolite. The plagioclase does not have a significant lamination. Megacrysts of plagioclase and Al-orthopyroxene that are so characteristic of massif-type anorthosite complexes also occur throughout the outcrop.

Oikocrystic textures similar to that of the Nodular Troctolite are commonly thought to imply a very low nucleation density of the oikocryst phase, here olivine. However, if this texture was produced by nucleation in a uniform medium at very low undercoolings then a random distribution of oikocrysts would be expected, which is not observed. It will be shown later that the plagioclase crystals have been coarsened and hence it is

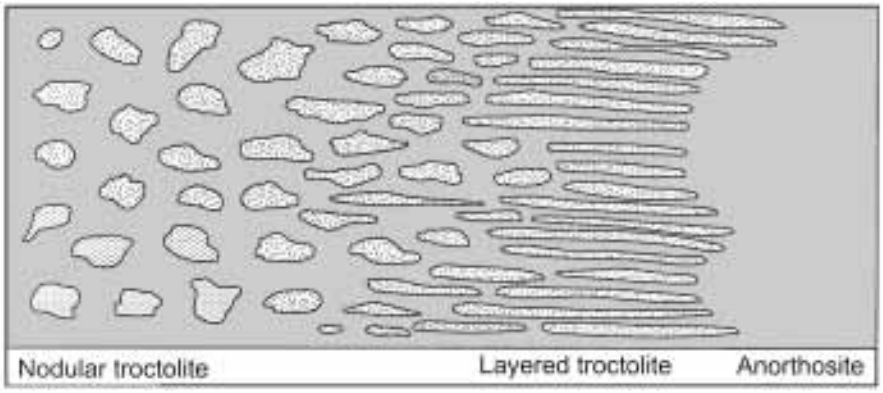

Fig. 1. Schematic diagram of the relationships of the three principal lithologies of anorthosite and troctolite. The section is ~1 m thick, but the horizontal scale is not linear. To the left the Nodular Troctolite consists of olivine oikocrysts 20–30 cm long (pale) set in a matrix of anorthosite with crystals 5–10 mm long (dark). The plagioclase chadocrysts in some oikocrysts are foliated (bottom left), but are more commonly massive. This texture is transitional to Layered Troctolite (centre) over a distance of a few metres to tens of metres. Layers are spaced 3–10 cm apart. Both plagioclase and olivine are 5–10 mm long. The Layered Troctolite terminates abruptly along sinuous boundaries against Massive Anorthosite, which has a texture similar to anorthositic patches in both types of troctolite.

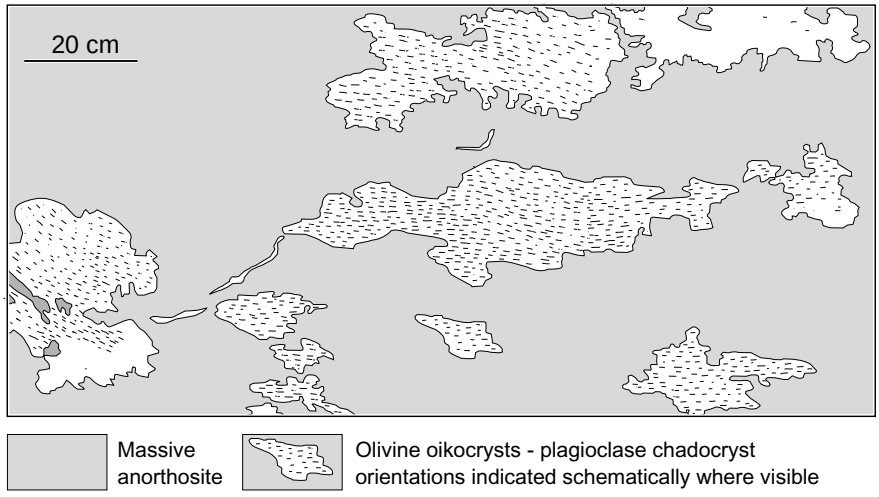

Fig. 2. Tracing of a series of photographs of an outcrop of Nodular Troctolite. The dark background is the massive anorthosite and the pale areas are the olivine oikocrysts. Plagioclase chadocryst orientations in the oikocrysts are shown schematically where visible.

possible that the oikocrysts were coarsened also. Such a process can develop periodic patterns with layers (Boudreau, 1987) or more complex distributions (Ortoleva, 1994).

Most of the textures described here are difficult to interpret as only the final stage is preserved. However, for the Nodular Troctolite the oikocrysts have preserved a record of textural development. The rest of this paper will be devoted to quantitative textural examination of the development of this rock. A laminated part of the Nodular Troctolite has been chosen as this further constrains the development of the texture (Fig. 3).

NODULAR TROCTOLITE

The Nodular Troctolite is composed only of the two essential minerals, olivine and plagioclase. Olivine is only present as oikocrysts. It is not deformed or extensively altered, but near the edges of the oikocrysts it may have narrow rims of orthopyroxene. The olivine is unzoned, with 20 microprobe analyses in the range Fo 69 $\pm$ 2%, which is close to the analytical error at 95% confidence.

Plagioclase crystals within the oikocrysts and the matrix have strikingly different shapes, sizes and orientations. However, more than 200 microprobe analyses of plagioclase compositions indicate that there is no systematic

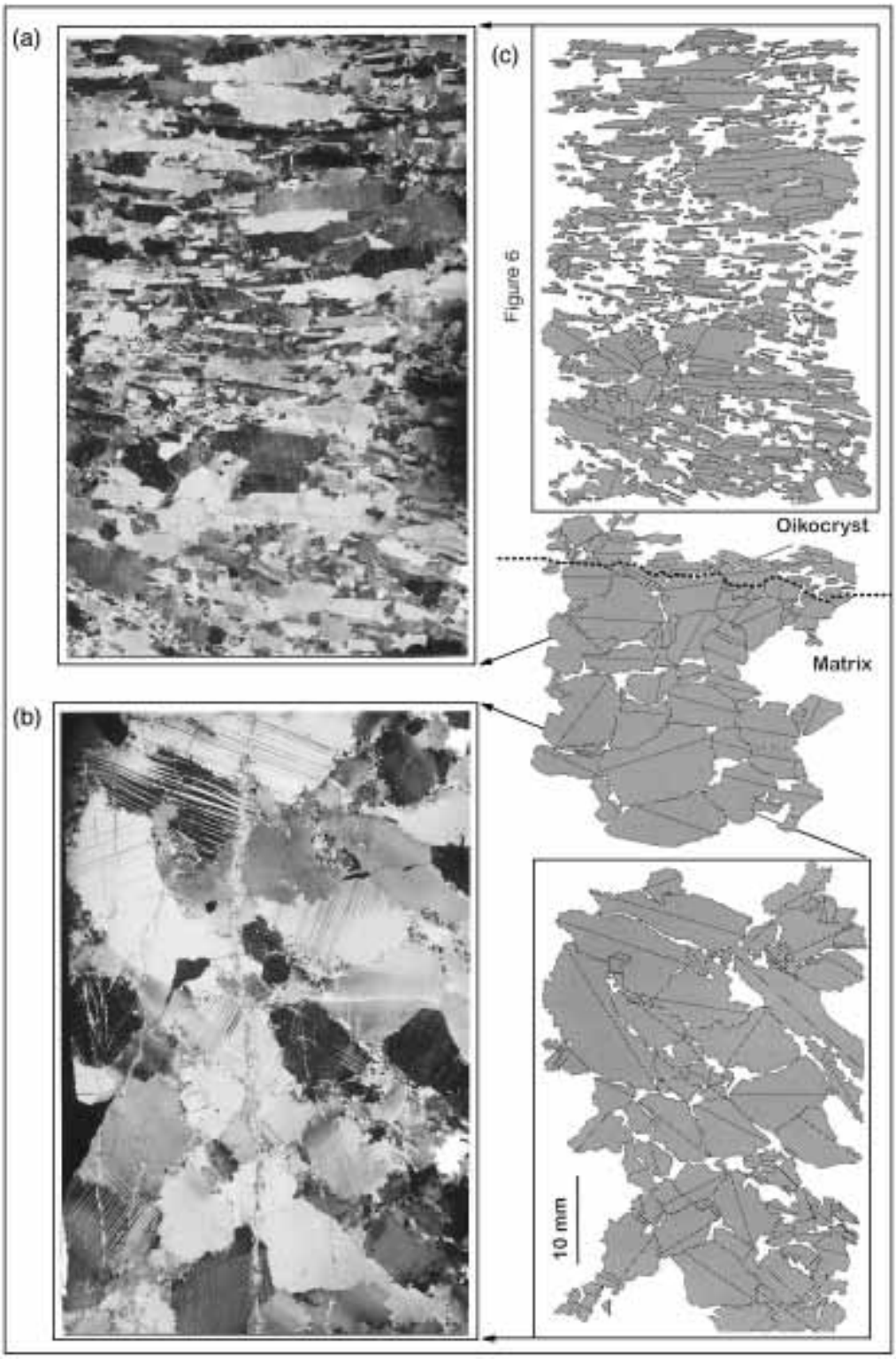

Fig. 3. The Nodular Troctolite. (a) Thin section of the matrix in cross-polarized light. The edges of the plagioclase crystals have been granulated during post-solidification deformation. A narrow vertical zone of scapolite alteration that cuts across the section was produced during Cambrian rifting. (b) Thin section of an olivine oikocryst adjacent to section (a) in cross-polarized light. The section is normal to the foliation and in the same plane as (a). (c) Section from the interior of an oikocryst into the matrix, digitized from photographs of three large thin sections, parts of two of which are shown in (a) and (b). This image is of the outlines of the plagioclase crystals as used for the quantitative textural analysis. The line within each crystal outline is parallel to the trace of the albite twin lamellae. Incomplete crystals at the edges of the thin sections have been omitted.

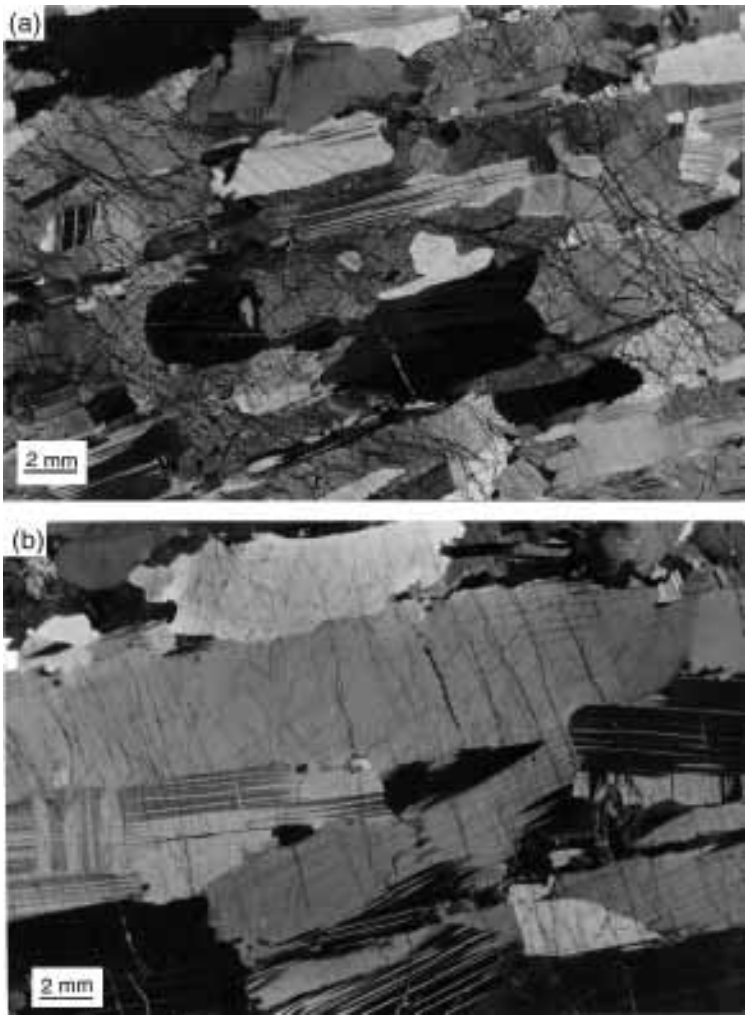

Fig. 4. Details of the textures within the oikocryst. All photographs are normal to the foliation and in cross-polarized light. (a) Many plagioclase crystals have retained their euhedral shape, although in some there is a little rounding. This may be due to the coarsening process (see text). (b) Some areas of the oikocryst contain a much larger proportion of chadocrysts and a larger grain-size. The strong lamination of the less chadocryst-rich areas is retained here.

compositional difference between the cores of those crystals in the oikocryst and in the matrix, with 90% of analyses falling in the range 62 $\pm$ 4 % An. The analytical error was estimated to be 2% at the 95% confidence level.

Plagioclase crystals in the oikocryst are euhedral to subhedral and are undeformed, displaying only albite twins (Fig. 4a). Plagioclase crystals are larger in areas of the oikocryst with a higher proportion of plagioclase (Fig. 4b). Most crystals are unzoned. Most plagioclase crystals are well aligned in the oikocryst.

In a few crystals near the edge of the oikocryst plagioclase occupies a space within the olivine that has the shape of a euhedral crystal of plagioclase, but the traces of the albite twin lamellae are oblique to the edge (Fig. 5a, b). There is no compositional difference between these new crystals and the others in the oikocryst. This morphology indicates that the original plagioclase crystal has been replaced by a new crystal with a different orientation. These crystals probably grew in from the matrix outside the oikocryst.

Plagioclase in the matrix is coarse grained and laminated, but the quality of the lamination is not as good as that of the plagioclase crystals in the oikocrysts (Fig. 3a). Plagioclase crystals are generally unzoned, except for sporadic, narrow reversely zoned rims. Similar rims have been found in anorthosites of the Kiglapait intrusion, Nain, and in massif-type anorthosites elsewhere (Morse & Nolan, 1985). A number of origins have been put forward, including the proposal by Morse & Nolan (1985) that they formed by crystallization of late trapped liquids, enriched in calcic components rejected by earlier

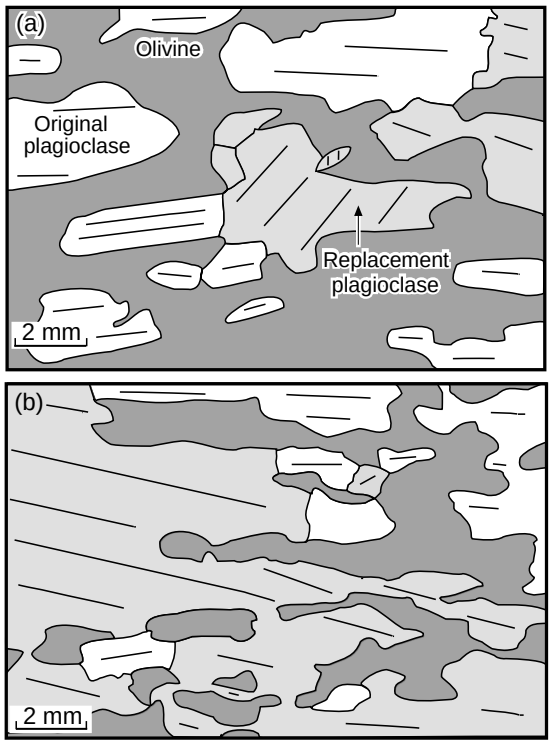

Fig. 5. Crystal replacement textures in plagioclase crystals (pale) within the olivine oikocryst (dark). Sections are normal to the foliation and in cross-polarized light. They were traced from photographs. (a) The plagioclase crystal in the centre left has a euhedral shape and the trace of the albite twin lamellae is parallel to the edges of the crystal. To the right an extension of this euhedral hole is occupied by another plagioclase crystal with a different orientation, where the trace of the albite twin lamellae is inclined at 45° to the long edge. The crystal on the left is early primocryst, which was being replaced by the crystal to the right (stippled) when the rock solidified. The latter is larger, and hence has a lower surface energy (see text). (b) An area of coarse plagioclase is in contact with an area that is less rich in chadocrysts. The shape of the olivine chadocryst in the centre indicates that small, euhedral plagioclase tablets were originally present. However, growth of the larger plagioclase crystal to the left has replaced these crystals with new plagioclase, with the trace of the twin plane of the albite twin lamellae inclined to the edge of the original crystals.

plagioclase crystallization. Hence their presence here indicates a lack of major grain-boundary movement in the sub-solidus state. A slightly modified explanation will be suggested later.

The origin of the lamination must now be discussed, even though it is not the focus of this paper, as it may have implications for the development of other aspects of the texture to be quantified later. Higgins (1991) and others have shown that flow of a crystal–liquid is a very efficient way to produce a well-developed foliation—compaction cannot produce significant foliation unless accompanied by very extensive recrystallization (Meurer, in preparation). The lack of wrapping of the foliation around the oikocrysts indicates that compaction, if it occurred, must have been very early. Higgins considers that the foliation was dominantly produced by flow, as it is the more efficient mechanism, but early compaction cannot be ruled out.

Plagioclase crystals in the matrix are commonly slightly deformed, with pericline and albite twins, and some edges are finely granulated, giving a protoclastic texture. The absence of granulation in the oikocrysts, even at plagioclase–plagioclase contacts, shows that deformation followed crystallization of the oikocrysts, and hence occurred after the processes to be discussed here. It was probably produced by late settling or movements of the intrusion or the emplacement of adjacent intrusions. Some plagioclase crystals in the oikocrysts are slightly deformed and the olivine oikocrysts have started to develop sub-grains, indicating that the oikocrysts were not totally immune to the late deformation observed in the matrix.

CRYSTAL SIZE, SHAPE AND ORIENTATION DISTRIBUTIONS

Three large thin sections were cut in a line from the centre of an oikocryst into the adjacent matrix for textural analysis (Figs 3 and 6). Photographs of the sections were enlarged to 30 cm × 45 cm and the outline of each plagioclase crystal in the photograph was traced by hand onto a digitizing tablet, after verifying the actual outline in the thin section with a polarizing microscope. All crystals in the thin section of the oikocryst were measured, as none were smaller than the minimum size that could be recognized in the photograph (0·25 mm). In the matrix, crystals smaller than 0·5 mm that lie along the grain boundaries of the larger crystals were interpreted to have been produced by cataclasis and were not measured. The raw positional data from the digitizing tablet were reduced to morphometric parameters using a program written by the author, and the reduced data were analysed with a spreadsheet program.

Stereology—conversion of 2D data to three dimensions

The raw data on crystal sizes are only a measurement of intersections of crystals with a plane (Table 1). Clearly, 3D size data are required for discussion. The stereological problem of conversion of 2D data to three dimensions is not simple for objects more geometrically complex than a sphere, and space does not allow it to be discussed in detail here [see, e.g. the review by Royet (1991)]. However, three aspects of the problem are relevant here.

(1) For a monodisperse population (one 3D size) of identical shapes the most common 2D long axis is less than the true 3D long axis (Fig. 7). This is known as the

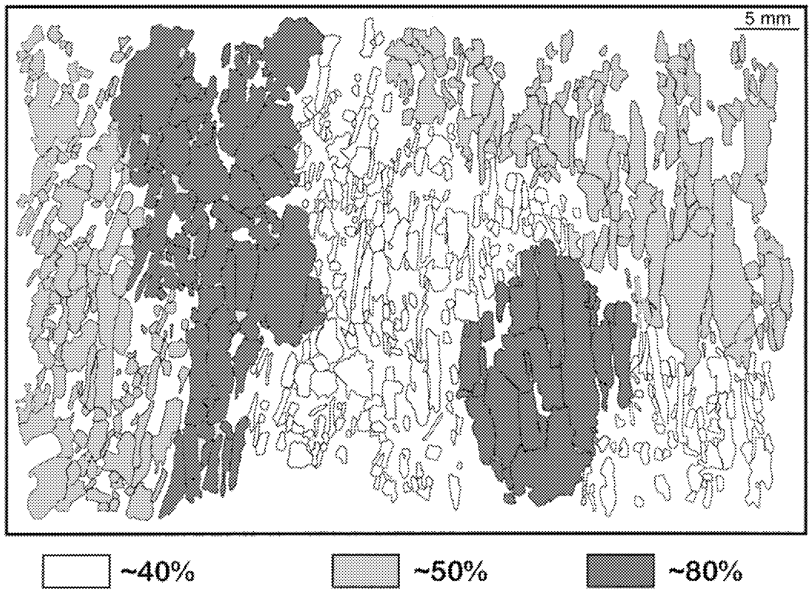

Fig. 6. Enlargement of the oikocryst shown in Fig. 3. Only plagioclase crystals are shown. The tones of the crystals correspond to regions with different proportions of plagioclase. These areas are interpreted to correspond to different degrees of solidification of the rock when the plagioclase crystals were isolated from the magma by growth of the oikocryst.

Table 1: Numbers of crystals in each size interval, areas and crystal shapes; size intervals are logarithmic

Upper limit of interval (mm)	Matrix	Oikocryst		
		~80% plagioclase	~50% plagioclase	~40% plagioclase
0·25–0·40	1	2	3	6
0·63	5	7	19	37
1·00	10	8	54	72
1·58	15	18	60	70
2·51	24	16	54	59
3·98	21	19	39	39
6·31	21	18	28	15
10·00	10	11	11	8
15·85	9	4	5	0
25·12	4	1	0	0
Total crystals	120	105	273	308
Area (mm^2)	1780	861	1358	998
Crystal shapes	1:1:1	1:3:3	1:3:3	1:3:3

cut section effect (Royet, 1991). There have been a number of studies of this problem for various geometrical shapes, but the shape most relevant for the case of plagioclase is the rectangular parallelepiped. Higgins (1994) showed that for randomly distributed crystal orientations (massive texture) the most likely intersection is the intermediate dimension. That is, for a crystal 1 mm × 2 mm × 10 mm it is 2 mm. The same argument can also be applied to polydisperse populations (many 3D sizes). This effect can be compensated for if the length axis of crystal size diagrams is considered to be the length of the intermediate axis. It can, of course, be readily converted to the true length if the crystal shape is known. Crystal shapes can be measured using separated crystals or estimated from distributions of intersection width/length ratios (Higgins, 1994).

(2) For a polydisperse distribution smaller crystals are less likely to be intersected by a plane than larger crystals. This is known as the intersection probability effect. Again, the problem is easily resolved for a monodisperse collection of spheres (Royet, 1991):

$$n_V = \frac{n_A}{D} \quad (1)$$

where n_V is the total number of spheres per unit volume, n_A is the total number per unit area and D is the diameter of the spheres. This relationship can be modified so that it applies to polydisperse collections of other shapes (Higgins, 1994; Peterson, 1996).

However, another conversion is dimensionally also possible:

$$n_V(L_{12}) = n_A(L_{12})^{1.5}/(L_2 - L_1) \quad (2)$$

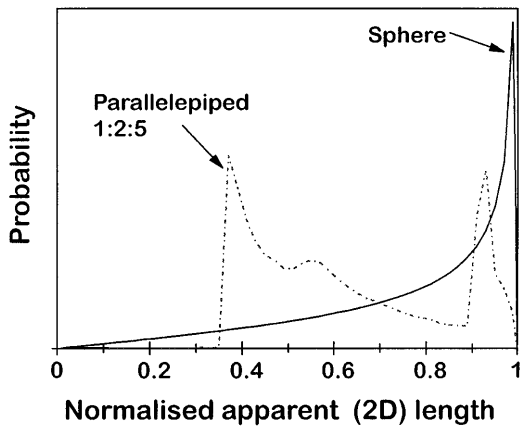

Fig. 7. Distribution of 2D intersection lengths normalized to the maximum intersection length for equal numbers of intersections. Simple shapes such as spheres have a single peak close to the maximum, but shapes closer to that of natural plagioclase, such as rectangular parallelepipeds, have multiple peaks. In this case, the mean intersection length is close to the intermediate dimension of the block (i.e. two for a block with dimensions 1:2:5).

where $n_V(L_{12})$ is the total number of crystals per unit volume in the length interval L_1 to L_2 (the population density), and $n_A(L_{12})$ is the total number of crystals per unit area in the length interval L_1 to L_2. This equation is the simplest way to convert the dimensions of $n_A(L_{12})$, L^{-2}, to those of $n_V(L_{12})$, L^{-3}. This conversion is much more commonly applied than equation (1) and will be used here for consistency [see review by Cashman (1990)]. The different equations give slightly different shapes to the CSDs, but affect all CSDs similarly.

(3) Intersection lengths (2D) in a monodisperse population cover a broad range about the modal length, with a maximum equal to the greatest 3D length. This is another aspect of the cut section effect. Therefore, for a polydisperse population the 3D distribution of lengths can only be found by applying the function for a monodisperse population of the same shape to the 2D length distribution. Unfortunately, the form of this function is known analytically only for spheres; shapes such as parallelepipeds must be derived numerically and can be very complex with several modes (Fig. 7; Higgins, 1994). There have been many attempts to resolve this problem (Royet, 1991). Some workers have used the shape distribution function directly, either for spheres (e.g. Armienti *et al.*, 1994) or for more complex shapes. This method works well for spheres and near-equant objects because the modal 2D length lies close to the maximum 3D length (Fig. 7). However, it fails for complex objects because the largest 2D intersections are not very common [see point (1) above]. That is, the modal 2D length is much less than the maximum 2D length. Hence, the less abundant, and less accurately determined, larger intersections are used to correct for the most abundant intersections, introducing large errors in the corrected 3D length distributions. If the modal length, rather than the greatest length, is used then the correction is much less important and can be neglected to a first approximation.

Some workers have used an empirical approach that solves all three problems. Known 3D distributions have been sampled in two dimensions and the relationship between the two numerically modelled. Some success has been achieved for CSDs that have a logarithmic–linear 3D crystal size distribution (Peterson, 1996), but the method cannot be generally applied to non-linear distributions such as those seen here without introducing unacceptable errors (see later).

Equation (2) will be used here to convert the data to 3D number densities. The length in this equation is the intermediate dimension of the crystals. It should be noted that other workers use different conversions. Remembering this, and the possibilities of advances in the solution of these problems in the future, the raw 2D data are presented in Table 1, together with the areas and crystal shapes, so that the data can be readily recalculated.

Results

Population densities were plotted on a ln (population density) vs length diagram (Fig. 8) following Marsh (1988). Logarithmic length intervals were used such that each size interval is $10^{0·2}$ larger than the previous bin. Each bin used in the discussion contains at least one crystal and there are no gaps with empty bins. The principal source of error at each point in this diagram is the counting statistics. All bins between 0·4 and 10 mm have significant numbers of crystals and hence errors are small on the logarithmic scale of population density. Outside these limits precision is worse, but still does not invalidate the data. To facilitate discussion of the data, the section of the oikocryst was divided visually into areas with different proportions of plagioclase—40, 50 and 80% (Fig. 8; Table 1). There values were chosen empirically to give useful sub-populations of crystals.

The CSDs of each area of the oikocryst and of the matrix are all convex upwards, and the shape and position of the curve vary systematically with solidification. The position of the maximum of the CSD increases from 0·7 mm in the 40% plagioclase area to 2·0 mm in the matrix (Table 2; Fig. 8). It should be noted that the cut-off for small crystals in the matrix (see above) was 0·5 mm, considerably smaller than the observed maximum, 2 mm, hence the convex-upwards shape of the matrix CSD is not an artefact of measurement. This effect is not a consideration for the oikocryst CSDs as all crystals in the thin section were measured.

There are not sufficient data to the left of the CSD maximum to determine if this section is linear, but overall

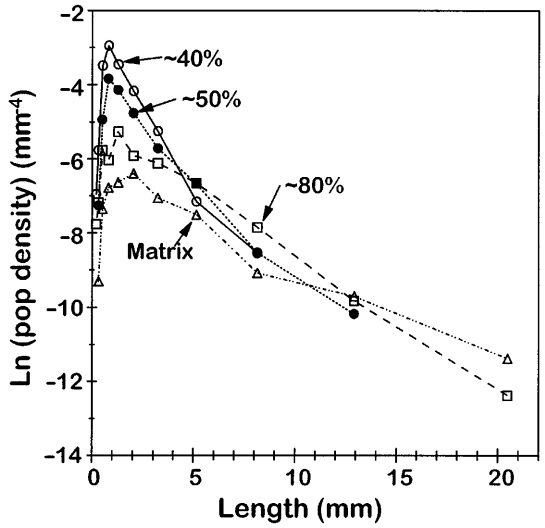

Fig. 8. Crystal size distribution (CSD) diagrams. CSDs within the oikocryst have been divided into regions of 40, 50 and 80% plagioclase (see text and Fig. 6). The minimum size of crystals measured is 0·25 mm for those within the oikocryst and 0·5 mm for those in the matrix.

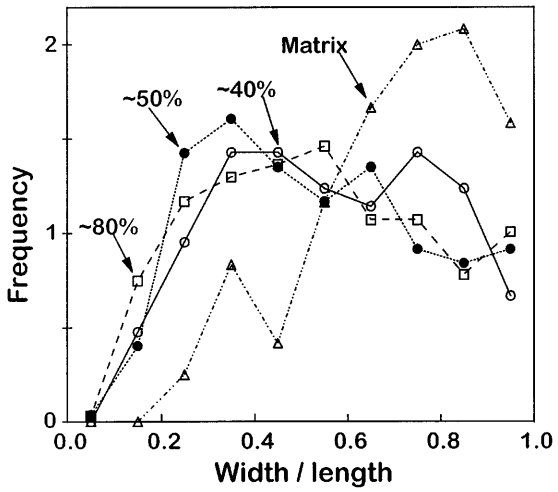

Fig. 9. Width/length distribution diagrams for the oikocryst and matrix plagioclase (see caption of Fig. 6). Frequency has been normalized so that the mean value is one. There is a clear difference in shape between the plagioclase in the oikocryst and in the matrix.

steepness decreases with increasing solidification within the oikocryst. The matrix appears to continue this trend, but less precisely and with the same caveat as above. The parts of the CSDs to the right are broadly linear, considering the errors associated with the population density of the largest crystals. The intercept and slope of a regression of these data both decrease with increasing solidification (Table 2; Fig. 8). The overall effect for the three areas of the oikocryst is rotation of the line around a point at 4 mm.

Higgins (1994) has shown that crystal shapes can be estimated from the distributions of width/length ratios of crystal outlines. The width/length distributions of plagioclase from all three areas of the oikocryst are similar, with a mode at about 0·35 and a skewness ((mean – mode)/standard deviation) of 0·82 (Fig. 9). These values indicate an overall aspect ratio for the crystals of 1:3:3 (Higgins, 1994). The width/length distribution of the matrix plagioclase is very different: the mode of 0·8 and skewness of –0·76 indicate almost equant crystals, but it is impossible to give exact dimensions (Higgins, 1994).

The orientation of the plagioclase crystals is defined by the trace of the albite twin planes. For most crystals the long axis in sections is parallel to the albite twin planes, hence both lattice-preferred orientations and shape-preferred orientations are identical. Within the oikocryst large plagioclase crystals are confined to a narrow range of orientations (Fig. 10), but crystals <2 mm long are more widely distributed, although still with a concentration around 0°. The plagioclase in the matrix is not nearly so well aligned (Fig. 10). The larger crystals have a mean orientation near 45°, reflecting undulations of the foliation direction visible in the outcrop (Figs 2 and 3). Crystals smaller than 7 mm are almost randomly oriented.

Table 2: Crystal size distribution parameters

% plagioclase	2D crystal number density (mm^{-2})	Mean crystal size (mm)	CSD Maximum (mm)	Regression of data on the right side of the CSD			
				Intercept [ln (mm^{-4})]	Slope (mm^{-1})	*R*	Number intervals
~40	0·306	1·73	0·7	−2·44 ± 0·37	−0·81 ± 0·05	0·982	6
~50	0·199	2·37	1·0	−3·54 ± 0·54	−0·60 ± 0·05	0·964	7
~80	0·120	3·57	1·5	−4·85 ± 0·13	−0·37 ± 0·02	0·994	7
Matrix (100)	0·067	4·26	2·0	−6·29 ± 0·54	−0·26 ± 0·03	0·938	6

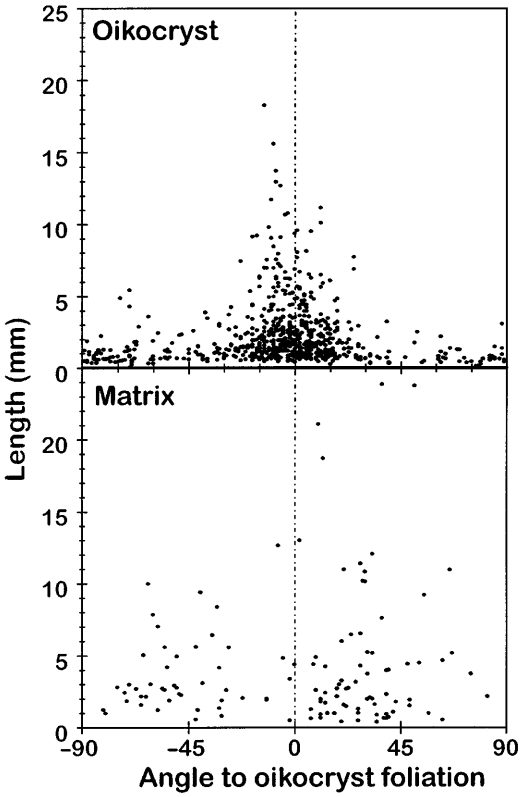

Fig. 10. Orientations of the trace of albite twin lamellae in plagioclase. All data for the oikocryst have been plotted together. There is a well-defined foliation in the oikocryst defined by many crystals. In the matrix the foliation is mostly defined by a few large crystals, and is parallel to that in the oikocryst.

DISCUSSION

Introduction

The most important assumption of this study is that the shapes of the plagioclase crystals are not significantly modified after they have been engulfed by the olivine oikocrysts. A further assumption is that the amount of plagioclase in a given volume increases at the same time as the oikocrysts grow, or at the very least does not decrease. These ideas seem reasonable and, as indicated in the Introduction, have been adopted by other researchers. Hence, the parts of the oikocryst that contain 40% plagioclase represent the texture when the system was 40% solidified, and will now be referred to in that way. The continuity of the lamination direction between the different oikocrysts can only be explained if the material between the oikocrysts (i.e. matrix) initially had a texture similar to that within the oikocrysts. This can be generalized to indicate that all the textures developed sequentially, in order of solidification (percentage plagioclase). For example, the matrix textures (100% solidified) passed through the 40, 50 and 80% solidification textures.

The simplest possible analysis of the textures, based only on crystal number density (number of crystals/volume) indicates that textural development can be divided into two periods (Table 1). The first was one of production of crystals by nucleation and growth, and hence increasing crystal number density. It was complete before 40% solidification, which is the earliest recorded texture. It is roughly equivalent to the primary textural development period of Hunter (1996). The second phase was of reduction in the crystal number density, but with a concurrent increase in mean grain size, resulting in an overall increase in the proportion of plagioclase until the rock was completely solidified. This process is termed textural coarsening, Ostwald ripening (Voorhees, 1992), crystal ageing (Boudreau, 1995) or competitive particle growth (Ortoleva, 1994). This phase is equivalent to the secondary textural development period of Hunter (1996).

Initial plagioclase nucleation and growth

Obviously, the crystallization of a magmatic rock must start with nucleation and growth of crystals. Marsh (1988) has applied CSD theory developed for industrial processes to petrology and has shown that on a graph of ln $[n_V(L)]$ vs L straight CSDs can be expected for both open-system and closed-system (batch) crystallization. For a closed system the logarithmic–linear correlation is produced by exponentially increasing nucleation with time, as would be produced if the undercooling of the magma was increasing linearly (Fig. 11a). For such relatively small undercoolings the maximum growth rate is rather high, although difficult to quantify. In batch crystallization crystal size can be correlated with crystal age, although the relationship is only linear if the growth rate is constant. Therefore, in a CSD diagram nucleation density is proxied by population density and time is proxied by length.

At 40% solidification the CSD is linear, except for small crystal sizes (see later), implying that crystallization occurred in an environment of linearly increasing undercooling (Figs 8 and 11a) In this part of the section both medium-sized and large crystals are well aligned (Figs 3 and 10), hence the magma must have been sheared or flowed as a slurry during crystallization, as compaction cannot produce such a pronounced lamination (Higgins, 1991). Crystallization produces latent heat, which must be removed if the undercooling is to increase. Nucleation and growth in a flowing or circulating magma provide a mechanism to remove such heat. The more dispersed orientations of the smaller crystals indicated that flow may have ceased towards the end of this period (Fig. 10).

The smallest grains are deficient as compared with a linear regression of the rest of the CSD data (Fig. 8). This could be due to a reduction of the nucleation density

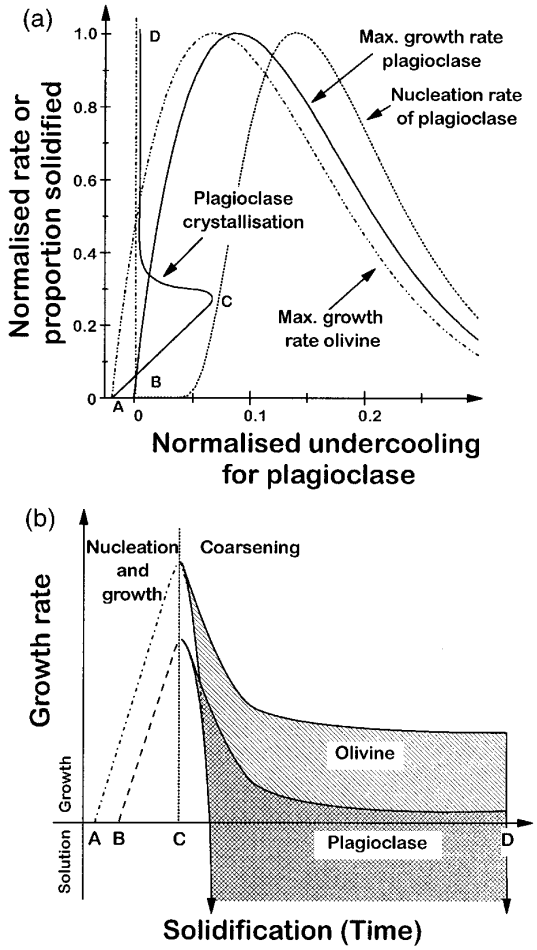

Fig. 11. (a) Schematic diagram of percentage solidified, maximum growth rate and nucleation rate vs undercooling. All values have been normalized to maximum values. Equations for growth and nucleation rates are the standard equations for interface-dominated systems (e.g. Cashman, 1990). Olivine first crystallized at A, followed by plagioclase at B. Nucleation and crystallization continued during a period of increasing undercooling. At point C, when the rock was at ~25% solidification, plagioclase undercooling decreased to very low values and coarsening started. Plagioclase grew at much lower rates than olivine: 0·1 vs 0·5 in this illustration. New material was also crystallized until the rock was completely solid at point D. (b) Olivine and plagioclase growth rate vs solidification. Olivine and plagioclase first appeared at points A and B. During the period of increasing undercooling (to point C) the growth rate of all olivine crystals was the same, no matter what their size. Plagioclase behaved in a similar way. During the coarsening period (from C to D) there was a range in growth rates: small crystals dissolved (negative growth rates) whereas larger crystals grew, albeit a little slower than during the first period (A to C).

during the last stages of crystallization or resorption of the smallest grains after their growth (see discussion of coarsening later). If the shapes of the CSDs of the 40, 50 and 80% solidified areas are extrapolated visually then it appears that the turn-down began at about 25% solidification. Therefore, the first phase of nucleation and growth with increasing undercooling must have finished by that point. If the turn-down in the 40% solidified CSD is due to decreasing nucleation density, then this time must be one of transition to the coarsening phase, during which there was no nucleation. Otherwise the turn-down is simply the initial stage of coarsening.

It is not possible to determine if there was any significant compaction during this phase for the following reasons: there was sufficient magma present that crystals could move freely and hence none were bent; there were no solid objects around which the plagioclase foliation could be bent (compare Sept Iles intrusion; Higgins, 1991); and any foliation produced by compaction would have been swamped by that produced by flow.

Textural adjustment—coarsening

Polydisperse multiphase mixtures are not in their lowest energy state, because of excess interfacial energy. In such systems the mean grain size tends to increase so as to reduce the overall energy of the system [see review by Voorhees (1992)]. Grain size can only be reduced if energy is added, by deformation for example. Clearly, there can be no nucleation of new crystals of the phase that is coarsening during this process, although other phases could nucleate and grow.

Material is transferred from grains smaller than a critical radius by diffusion to the larger grains by several different mechanisms [see review by Hunter (1996)]. If there is no magma present then diffusion may be within the body of the grains or, more likely, along grain boundaries. If a magma is present then diffusion in the magma dominates any within-grain diffusion. Reversed rims on some plagioclase crystals imply that magma was present, at least between some grains, during the production of the textures observed here (except the final granulation). Such rims also indicate that there have not been any major grain-boundary movements in the subsolidus.

Although the thermodynamic driving forces of the process are well known and understood, the kinetics are complex and the subject of much research, especially in the field of material sciences (Voorhees, 1992). Unfortunately, the number of variables is very large and most of the systems investigated are not appropriate to geological conditions. Nevertheless, a good starting point is the earliest and most well-known solution, that formulated by Lifshitz & Slyozov (1961) and others, known as the Lifshitz–Slyozov–Wagner (LSW) theory. The solution is for dilute systems; that is, there is assumed to be no interaction between crystals—all communicate directly with a uniform fluid. The crystals are assumed to be spherical. Most applications of LSW theory (and modifications of the theory) have been concerned with

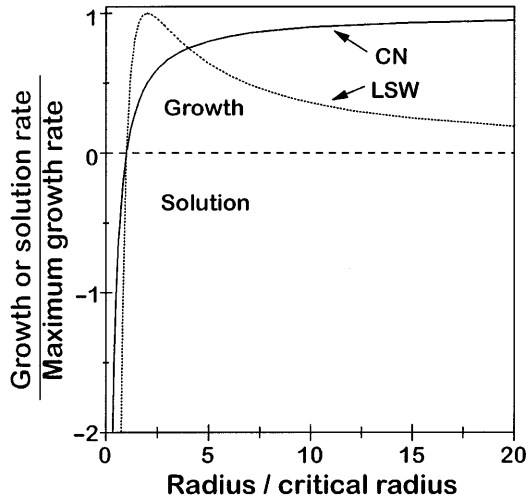

Fig. 12. Normalized growth rate variations for the Lifshitz–Slyozov–Wagner (LSW) equation [equation (3)] and the communicating neighbours (CN) equation [equation (4)]. It should be noted that the growth rate predicted by the LSW theory tends to zero for large crystals, whereas that predicted by the CN theory tends to a maximum value.

the relationship between mean crystal size and time. However, in plutonic rocks solidification time is not well constrained. In these circumstances, an equation relating growth rate to crystal size is more interesting (Lifshitz & Slyozov, 1961):

$$\left(\frac{\mathrm{d}r}{\mathrm{d}t}\right)=\frac{k}{r}\left(\frac{1}{r^*}-\frac{1}{r}\right) \tag{3}$$

where $\mathrm{d}r/\mathrm{d}t$ is the growth rate, r^* is the critical radius, r is the crystal radius and k is a rate constant.

A graph of growth rate vs radius shows that crystals below the critical radius are strongly resorbed and their material is transferred to crystals slightly larger that the critical radius (Fig. 12). The growth rate of infinitely large crystals is zero. The rate constant k is dependent on temperature and its value is not known for plagioclase in this system.

The LSW equation for coarsening has been modelled numerically with a spreadsheet program. Eight thousand random numbers were manipulated mathematically so that their CSD resembled that of the 40% solidified texture, except that the CSD was linear to zero length. The modelling was done sequentially on this population. Time was non-dimensionalized with steps of 0·25, 0·5, 0·75 and 1·00. The constant k and the critical radii for each step were varied to try to achieve the best fit to the natural data. Figure 13a shows the results of this model. Clearly, it is easy to produce depletion of small crystals although not as strong as is observed. However, the slope of the right part of the CSD diagram does not decrease, as is observed in the rocks, but even increases a little. Increasing the value of k merely exacerbates this problem.

The limitations of the LSW equation are well known, hence it is not surprising that it is unable to model the observed CSDs. Numerous modifications have been proposed, such as extensions to high volume fractions [see review by Voorhees (1992)]. However, as DeHoff (1991) has pointed out: 'The literature abounds with theoretical treatments of coarsening for an additional important reason: the existing theories do not work.' DeHoff proposed a new theory, which he called the communicating neighbours (CN) theory.

CN theory is based on the observation that in many laboratory studies the growth rate of each crystal is not solely controlled by its size, but appears to be characteristic of each crystal, an effect called growth rate dispersion. This suggests that the position of each crystal is important during growth and hence that crystals communicate with each other and not only with some uniform fluid. Of course, the mechanism for communication, as in the LSW theory, is by diffusion. DeHoff (1991) has formulated a geometrically general theory using this principle. The most readily applicable equation relates growth rate and crystal radius:

$$\left(\frac{\mathrm{d}r}{\mathrm{d}t}\right)=k\left\langle\frac{1}{\lambda}\right\rangle\left(\frac{1}{r^*}-\frac{1}{r}\right) \tag{4}$$

where $\mathrm{d}r/\mathrm{d}t$ is the growth rate, k is a rate constant (different from that in the LSW theory), $\langle 1/\lambda\rangle$ is the harmonic mean of the intercrystal distance, r^* is the critical radius and r is the crystal radius. This equation illustrates the fundamental difference between the LSW and CN theories: in the former the diffusion length scale is a property of the particle itself, hence the $1/r$ dependence, whereas in the CN theory it is dependent on the distances to the neighbouring particles. This equation is for crystal growth controlled by diffusion. A similar equation also applies to interface-controlled growth (DeHoff, 1984).

A graph of growth rate vs radius for the CN equation shows that crystals below the critical radius are resorbed rapidly, although less so than with the LSW equation (Fig. 12). The major difference is for crystals larger than the critical radius, where the growth rate increases asymptotically with radius. This equation is much more interesting than the LSW equation, as the growth rate is constant for crystals much larger than the critical radius, and will then depend on undercooling, amongst other factors (Fig. 12).

The harmonic mean may be evaluated using

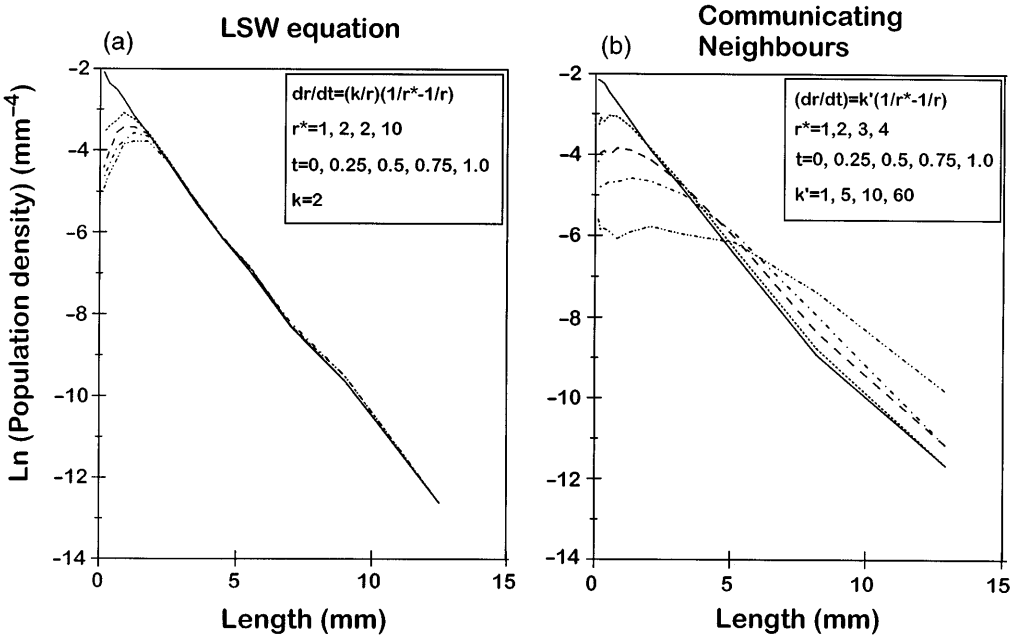

Fig. 13. Modelling of CSD variations with (a) Lifshitz–Slyozov–Wagner and (b) communicating neighbours equations. The initial model ($t = 0$) is based on 8000 pseudo-crystals with a CSD similar to that of the 40% solidified areas of the oikocryst (see text).

$$\left\langle \frac{1}{\lambda} \right\rangle = \alpha n_V^{1/3} \tag{5}$$

where α depends on the nature of the distribution and has a value of 2·18 for a Poisson distribution. The population density (n_V) observed here varies by a factor of four, translating to a variation in $\langle 1/\lambda \rangle$ of only 1·6. Therefore, this variable can be combined with the rate constant k into a new constant k'.

Sequential modelling similar to that used for the LSW equation was applied to the CN equation (Fig. 13b). Again, the critical radius and modified rate constant (k') were varied to achieve the best fit to the natural data. Although the smallest crystals are again depleted and the peaks of the CSDs better match the natural values, the turn-downs at small lengths are not as steep as observed. However, the match for the right side of the CSD diagram is much better: the slopes of the CSDs decrease and rotate about a point near 4 mm. It should be noted that the common practice of plotting linearly crystal population densities against length conceals the variations in the number of large crystals (e.g. Cashman & Ferry, 1988). Hence, the difference between the CN and LSW theories is not so clear on these diagrams.

These models indicate that plagioclase textures developed by textural coarsening, following the CN theory (DeHoff, 1991), but why did it occur? The first stage of solidification was one of increasing undercooling (Fig. 11). However, the increasing crystallinity (of both plagioclase and olivine) would have impeded the flow of interstitial magma. Latent heat could not be removed so easily, leading to a rise in temperature (lower undercooling) and suppression of nucleation (Fig. 11). Closer to the liquidus temperature of plagioclase the critical radius increased, hence allowing coarsening to occur by the destruction of small crystals and the growth of larger crystals.

The large size of the oikocrysts and the lack of smaller olivine crystals imply that olivine was also coarsened like plagioclase. Hence, it is proposed that the low population density of the oikocrysts is not a primary feature, but one developed during textural coarsening. The original population density of the olivine before coarsening may have been similar to that of the plagioclase, but is now inaccessible.

Other textures in the rocks near the Nodular Troctolite support the idea that locally olivine crystals smaller than a critical size may have been dissolved. The abrupt termination of the layered troctolite against the anorthosite is most easily explained by the solution of olivine, converting troctolite to anorthosite. Perhaps late circulating magmatic fluids were focused into these areas by locally higher permeability and the olivine of the troctolite, which was smaller than the critical size, dissolved in the magma. The olivine component of the magma could have re-entered the magma chamber or been precipitated to enlarge the oikocrysts. Similar discordant bodies have been observed in other layered mafic intrusions (e.g. McBirney & Hunter, 1995; Meurer *et al.*,

1997) and are generally considered to be the result of metasomatic processes. However, the grain size in many of these bodies is greater than that of their host rocks, hence textural coarsening may well be important. If the crystals in the metasomatic protolith are smaller than the critical size for the percolating magma, then they will dissolve, even if the chemical composition of the magma is not different from that which the crystals originally crystallized from. Hence, it may not always be necessary to propose magmatic fluids with different compositions to effect the observed changes in modal composition.

Coarsening can also provide a new explanation for the origin of the poikilitic texture. The classical theory proposes that the chadocryst phase nucleated and grew first. Subsequently, the oikocryst phase nucleated, grew faster than the chadocryst crystals and engulfed them. However, there is a problem that under plutonic conditions olivine or pyroxene commonly nucleates at higher temperatures than plagioclase. This is indicated by the common occurrence of olivine-rich cumulates at the base of layered intrusions. Let us assume, for the moment, that olivine did indeed nucleate and grow first (Fig. 12). As cooling proceeded plagioclase joined olivine and the two continued to nucleate and grow together. The texture at this point would consist of olivine crystals, some partly enclosed by plagioclase. Once coarsening started the texture changed dramatically. As mentioned above, once crystallinity interferes with magma circulation latent heat cannot be removed fast enough and the temperature will rise. The temperature will be buffered close to the liquidus temperature of plagioclase as solution of plagioclase will adsorb heat. However, at this temperature olivine is more undercooled than the plagioclase and will have a higher maximum growth rate (Fig. 11). The olivine crystals will coarsen and grow rapidly, engulfing the plagioclase. Evidence of the early crystallization of olivine may only be preserved at the centre of some oikocrysts, which are not volumetrically important, and hence will only be rarely seen. Hence, coarsening necessarily produces an apparent crystallization order that is the reverse of the order of nucleation of the phases. This process is not at odds with the original assumption of this study—that oikocrysts preserve the early textures of the chadocryst phases—as the coarsening of the olivine starts early in the solidification of the rock.

Means & Park (1994) have suggested that a number of textural processes that they observed in polyphase artificial systems might be applicable to igneous rocks. In particular, they found evidence for phase boundary migration that has changed the apparent order of crystallization. In this study the textural evidence indicates that the phase boundaries are resistant to change, as illustrated by the preservation of euhedral 'holes' in the oikocryst now occupied by new plagioclase crystals (Fig. 5). Hence, this aspect of their model is not applicable here. However, grain boundary migration, as they also observed, is clearly very important here.

One particularly striking aspect of the textural development is the loss of quality of lamination and change of crystal shape in the last developed textures (i.e. the matrix). This can be readily explained by the coarsening process in two ways. As the proportion of magma decreases the mechanism for diffusion must change also (Hunter, 1996). Initially, diffusion is mediated via the magma, but later diffusion must be partly restricted to grain boundaries, as within-grain diffusion will be slower still. Such a change in diffusive mechanism may affect the growth of different faces of the particle by changing the width of the chemical boundary layer. Another explanation is based solely on mechanical processes, as follows. As grains grow at the expense of their smaller neighbours their ends will meet neighbouring crystals before the sides. Hence growth on the sides will be less restricted and the grain will become more equant. There will also be rotation of individual crystals to accommodate better their new dimensions. This effect is particularly important when space is limited, for example, during the last stages of solidification. This process will steadily reduce the quality of the lamination, as there is no counteracting force, such as the original magmatic flow, to restore the original quality of lamination. Similar grain rotation has been observed in the experiments of Means & Park (1994).

Finally, textural coarsening may provide another explanation for the origin of reversely zoned rims on plagioclase. The cores of most plagioclase crystals are more An rich than the rims (normal zoning). Hence, as crystals smaller than the critical radius dissolve they will feed progressively more An-rich material into the residual magma, which in term will feed the growth of the larger crystals. When the rock is almost solid this effect could have an important influence on the last parts of the plagioclase crystals to form—the reversely zoned rims.

Other examples of textural coarsening

The same general pattern of textural coarsening as recorded here by the plagioclase CSDs can be seen in the CSDs of other minerals in different rocks.

A time-sequence of textural development was sampled in a drill-core that penetrated the upper part of the Makaopuhi lava lake (Cashman & Marsh, 1988). CSDs of samples with crystallinities from 20 to 80% have decreasing slopes and intercepts that pivot around a length of 0·1 mm (Fig. 14a). Cashman & Marsh (1988) considered that these textures were produced by crystallization under conditions of linearly increasing undercooling. Hence, the nucleation density decreased with increasing crystallinity. However, if it is assumed that

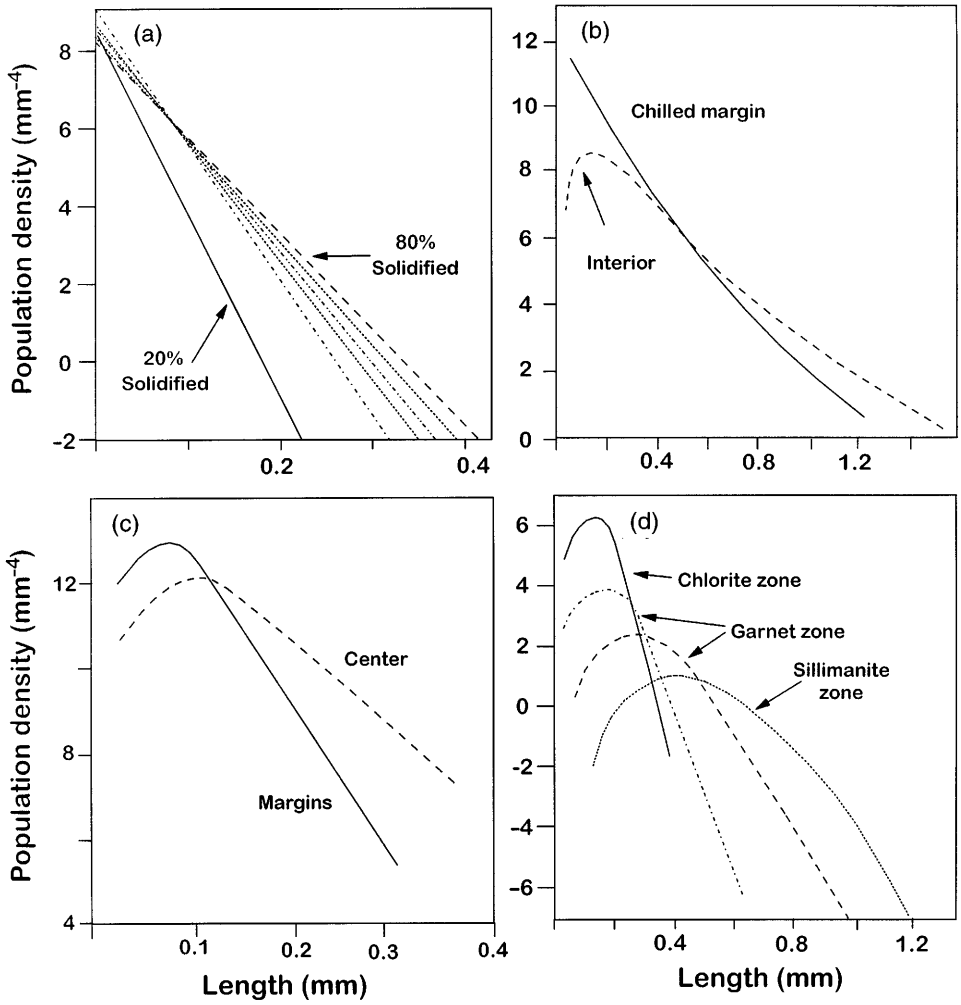

Fig. 14. Other examples of CSDs reflecting textural coarsening drawn from the literature. (a) Plagioclase in the Makaopuhi lava lake (Cashman & Marsh, 1988). (b) Clinopyroxene in the Box Elder intrusion, Montana (Resmini, 1993). (c) Chromites in the Stillwater complex (Waters & Boudreau, 1996). (d) Garnets in regionally metamorphosed rocks, Waterville formation, Maine (Cashman & Ferry, 1988).

crystals only grew, and there was no resorption, then the CSDs of the more solid samples should record the first period of increasing nucleation density, following by decreasing nucleation density as the crystallinity increased from 20 to 80%. Such a CSD would have a peak that would migrate to greater lengths as crystallization proceeded, keeping a constant height and slope on either side. This is not what is observed, hence there must be resorption of smaller crystals during the period 20–80% crystallized, as was observed in the Nodular Troctolite of the LSJAC. The CN coarsening theory can reproduce the observed rotation of the CSDs around a fixed point.

The Box Elder intrusion, Montana, is a 140 m thick laccolith of shonkinite (mafic syenite). The CSD of the clinopyroxene in the chilled margin is broadly linear with a slight curvature concave upwards, whereas the CSD from the interior is hump shaped with a shallower right-hand slope (Fig. 14b; Resmini, 1993). This feature closely resembles the coarsening observed in the Nodular Troctolite and was probably due to the same mechanism. The slight curvature of the chilled margin CSD suggests that coarsening had already started when the magma was chilled.

Another example of coarsening is shown by chromite cumulates in the Stillwater complex (Waters & Boudreau, 1996). Centimetric layers rich in chromite were examined. Even in thin section the crystals in the centre of the layer are clearly larger and more abundant. The CSDs confirm that the centre has been coarsened, compared with the edges (Fig. 14c). This behaviour is consistent with the DeHoff model of coarsening, as the growth rate will be higher where the crystal edges are

closer together. This type of positive feedback, reinforcing early, weak structures, has been explored by Boudreau (1987, and subsequent papers) and may account for the well-known 'inch-scale' layering in the Stillwater complex.

It is not surprising that metamorphic rocks also show evidence of coarsening. For instance, Cashman & Ferry (1988) have studied garnets in regionally metamorphosed rocks of the Waterville formation, Maine, from chlorite zone to sillimanite zone. The shape and behaviour of the CSDs exactly follow those expected for increasing coarsening with increasing metamorphic grade (Fig. 14d). That lower-grade rocks do not coarsen as much as those at higher grade suggests that there is some kinetic barrier limiting growth. This may be mineralogical or topological.

CONCLUSIONS

The following events are thought to have produced the textures observed in the Nodular Troctolite. The first phase to crystallize was olivine. It nucleated and grew in an environment of increasing undercooling. As the temperature dropped it was joined by plagioclase and the two continued to nucleate and grow together. At this time each phase had a linear CSD. The strong lamination of the early plagioclase indicates that the magma was flowing or being deformed at the time. Increasing undercooling was accommodated by removal of latent heat by the moving magma. Increasing crystallization impeded movement of the fluid component of the magma, hence latent heat could not be removed so readily. The temperature rose until it was just below that of the liquidus of plagioclase. There it was buffered by the solution and crystallization of plagioclase. At this temperature nucleation of both olivine and plagioclase was suppressed and textural coarsening started to occur. Small crystals were resorbed and larger crystals grew, both from recycled small crystals and new material in the magma. Both plagioclase and olivine were coarsened, but the largest olivine grains grew faster than the plagioclase as they were more undercooled. The olivine engulfed the plagioclase as it was coarsening and produced the poikilitic texture. Between the oikocrysts, plagioclase continued to coarsen until it had displaced all the magma. Maintenance of the temperature close to that of the first appearance of plagioclase for most of the duration of the crystallization prevented the nucleation and growth of other phases.

A number of other points are important:

(1) Coarsening appears to have followed more closely the communicating neighbours equation, rather than the more well-known Lifshitz–Slyozov–Wagner equation.

(2) There is no evidence for compaction during either the nucleation and growth stage or the textural adjustment stage. However, absence of evidence should not be construed as evidence of absence.

(3) The lamination of the plagioclase was developed early in the crystallization, but the quality of the initial lamination was reduced during the final stages of coarsening. This effect may be important in other rocks, and caution should be applied to the interpretation of fabrics or lack of fabrics in coarsened rocks.

(4) Reversely zoned rims on plagioclase may have formed by the solution of An-rich cores of smaller plagioclase crystals.

(5) The development of monomineralic rocks from more complex magmas requires expulsion of all liquid by compaction or the continuous flow of liquid through the system. In either case, textural coarsening will help keep magma channels open by removing small crystals that would have blocked them.

(6) Monomineralic areas of gabbros and troctolites may be produced by solution of mafic minerals that are smaller than a critical size. This mechanism should be important if adjacent rocks contain oikocrysts of the same minerals.

(7) Metasomatic replacement of minerals has commonly been proposed for the origin of discordant bodies in intrusions. Chemical differences between the rock and a percolating fluid destabilize some minerals and precipitate others. However, such bodies are commonly coarser than the host rock, hence crystal sizes may also play a role in the stability of phases. It may not always be necessary to propose a new and different magma to cause the observed mineralogical changes.

(8) The crystallization order of minerals in a rock is commonly determined and interpreted to be the same as their order of first appearance and nucleation. This is clearly not the case for coarsened rocks. Indeed, for two phases studied here the order is reversed.

(9) It is not surprising that textural coarsening can be seen in metamorphic and plutonic rocks (Fig. 14). However, if the same process is active in lava lakes then it might also be important in volcanic systems.

(10) Some pegmatites or areas of coarse crystals in plutonic rocks may have formed by extreme textural coarsening, rather than direct crystallization of late fluids, as is commonly supposed.

ACKNOWLEDGEMENTS

I would like to thank Josée Désgagne for digitizing the sections, Tobi Cohen for directing me to references on Ostwald ripening, Michel Hervet for help in the field, and Sarah-Jane Barnes for comments on a draft of this manuscript. Reviews by Tony Fowler, Bill Meurer, Alan

Boudreau and an anonymous reviewer helped improve the final manuscript. The Department of Geology, Université Blaise Pascal, Clermont-Ferrand, France, welcomed me during my sabbatical. This project was financed by a grant from the Natural Science and Engineering Research Council of Canada.

REFERENCES

Armienti, P., Pareschi, M. T., Innocenti, F. & Pompilio, M. (1994). Effects of magma storage and ascent on the kinetics of crystal growth. *Contributions to Mineralogy and Petrology* **115,** 402–414.

Boudreau, A. E. (1987). Pattern forming during crystallisation and the formation of fine-scale layering. In: Parsons, I. (eds) *Origins of Igneous Layering*. Dordrecht: D. Reidel, pp. 453–471.

Boudreau, A. E. (1995). Crystal aging and the formation of fine-scale igneous layering. *Mineralogy and Petrology* **54,** 55–69.

Cashman, K. V. (1990). Textural constraints on the kinetics of crystallization of igneous rocks. In: Nicholls, J. & Russell, J. K. (eds) *Modern Methods of Igneous Petrology: Understanding Magmatic Processes. Mineralogical Society of America, Reviews in Mineralogy* **24,** 259–314.

Cashman, K. V. & Ferry, J. M. (1988). Crystal size distribution (CSD) in rocks and the kinetics and dynamics of crystallization III. Metamorphic crystallization. *Contributions to Mineralogy and Petrology* **99,** 410–415.

Cashman, K. V. & Marsh, B. D. (1988). Crystal size distribution (CSD) in rocks and the kinetics and dynamics of crystallisation II. Makaopuhi lava lake. *Contributions to Mineralogy and Petrology* **99,** 292–305.

DeHoff, R. T. (1984). Generalized microstructural evolution by interface controlled coarsening. *Acta Metallurgica* **32,** 43–47.

DeHoff, R. T. (1991). A geometrically general theory of diffusion controlled coarsening. *Acta Metallurgica et Materialia* **39**(10), 2349–2360.

Higgins, M. D. (1991). The origin of laminated and massive anorthosite, Sept Iles intrusion, Quebec, Canada. *Contributions to Mineralogy and Petrology* **106,** 340–354.

Higgins, M. D. (1994). Determination of crystal morphology and size from bulk measurements on thin sections: numerical modelling. *American Mineralogist* **79,** 113–119.

Higgins, M. D. (1997). Origin of potassium-feldspar megacrysts in granitoids by textural coarsening: a quantitative study from the Cathedral Peak granodiorite, California. In: *Abstracts of Conference on Modern and Classical Techniques in Granite Studies,* Heulva, Spain, November, 1997.

Higgins, M. D. & van Breemen, O. (1992). The age of the Lac-St-Jean Anorthosite intrusion and associated mafic rocks, Grenville Province, Canada. *Canadian Journal of Earth Sciences* **29,** 1412–1423.

Hunter, R. H. (1996). Textural development in cumulate rocks. In: Cawthorn, R. G. (ed.) *Layered Intrusions. Developments in Petrology*. Amsterdam: Elsevier, pp. 77–101.

Jackson, E. D. (1961). Primary textures and mineral associations in the ultramafic zone of the Stillwater complex, Montana. *US Geological Survey Professional Paper* **358,** 106.

Lafrance, B., John, B. E. & Scoates, J. S. (1995). Syn-emplacement recrystallisation and deformation microstructures in the Poe Mountain anorthosite, Wyoming. *Contributions to Mineralogy and Petrology* **122,** 431–440.

Lifshitz, I. M. & Slyozov, V. V. (1961). The kinetics of precipitation from supersaturated solid solutions. *Journal of Physics and Chemistry of Solids* **19,** 35–50.

Maijer, C. & Padget, P. (eds) (1989). *The Geology of Southern Norway: an Excursion Guide*. Special Publication 1. Trondheim: Norges Geologiske Undersokelse.

Marsh, B. (1988). Crystal size distribution (CSD) in rocks and the kinetics and dynamics of crystallization I. Theory. *Contributions to Mineralogy and Petrology* **99,** 277–291.

Mathison, C. I. (1987). Pyroxene oikocrysts in troctolitic cumulates—evidence for supercooled crystallisation and postcumulus modification. *Contributions to Mineralogy and Petrology* **97,** 228–236.

McBirney, A. R. & Hunter, R. H. (1995). The cumulate paradigm reconsidered. *Journal of Geology* **103,** 114–122.

Means, W. D. & Park, Y. (1994). New experimental approach to understanding igneous textures. *Geology* **22,** 323–326.

Meurer, W. P., Klaber, S. & Boudreau, A. E. (1997). Discordant bodies from olivine-bearing zones III and IV of the Stillwater complex, Montana—evidence for post-cumulus fluid migration and reaction in layered intrusions. *Contributions to Mineralogy and Petrology* **130,** 81–92.

Morse, S. A. & Nolan, K. M. (1985). Origin of strong reversed rims on plagioclase in cumulates. *Earth and Planetary Science Letters* **68,** 485–498.

Ortoleva, P. J. (1994). *Geochemical Self-Organisation*. New York: Oxford University Press.

Peterson, T. D. (1996). A refined technique for measuring crystal size distributions in thin section. *Contributions to Mineralogy and Petrology* **124,** 395–405.

Resmini, R. G. (1993). Dynamics of magma in the crust: a study using crystal size distribution. Ph.D. Thesis, Johns Hopkins University, Baltimore, MD.

Royet, J.-P. (1991). Stereology: a method for analysing images. *Progress in Neurobiology* **37,** 433–474.

Voorhees, P. W. (1992). Ostwald ripening of two-phase mixtures. *Annual Review of Materials Science* **22,** 197–215.

Waters, C. & Boudreau, A. E. (1996). A reevaluation of crystal size distribution in chromite cumulates. *American Mineralogist* **81,** 1452–1459.

Woussen, G., Martignole, J. & Nantel, S. (1988). The Lac-St-Jean anorthosite in the St-Henri-de-Taillon area (Grenville Province): a relict of a layered complex. *Canadian Mineralogist* **26,** 1013–1025.